DYNAMIC MODELING AND FLIGHT CONTROL OF MORPHING AIR VEHICLES

By

KENNETH E. BOOTHE JR.

A THESIS PRESENTED TO THE GRADUATE SCHOOL
OF THE UNIVERSITY OF FLORIDA IN PARTIAL FULFILLMENT
OF THE REQUIREMENTS FOR THE DEGREE OF
MASTER OF SCIENCE

UNIVERSITY OF FLORIDA

2004

I dedicate this work to God and my loving and supportive parents to whom I owe all of my success.

ACKNOWLEDGMENTS

I would like to acknowledge the help and teaching of my professors, primarily Dr. Lind

TABLE OF CONTENTS

page

ACKNOWLEDGMENTS iv

LIST OF TABLES vii

LIST OF FIGURES viii

NOMENCLATURE x

ABSTRACT xi

CHAPTER

1 INTRODUCTION 1

2 MORPHING AIRCRAFT 5

2.1 History 5
2.2 University of Florida Micro Air Vehicles 6

3 MORPHING AIRCRAFT EQUATIONS OF MOTION 11

3.1 Nonlinear Equations of Motion 11
3.1.1 Angular Momentum 11
3.1.2 Force Equations 13
3.1.3 Attitude and Angular Velocities 14
3.2 Linearized Equations of Motion 15
3.2.1 Angular Momentum 15
3.2.2 Force Equations 17
3.2.3 Attitude and Angular Velocities 18
3.3 Straight and Level Flight 19

4 MODELING 22

5 CONTROL SYNTHESIS 24

5.1 Quasi-static Morphing 24
5.2 Dynamic Morphing 24

6 APPLICATION - BASE MODEL 27

6.1 Vehicle Description 27
6.2 Modeling 29

6.2.1 Aerodynamic Modeling - Tornado 29
6.2.2 Rigid Body Modeling-ProE 29

7 APPLICATION-VARIABLE SPAN 31

7.1 Vehicle Description 31
7.2 Flight Dynamics 31

8 APPLICATION-VARIABLE CAMBER 36

8.1 Vehicle Description 36
8.2 Flight Dynamics 37

9 APPLICATION-VARIABLE CHORD 41

9.1 Vehicle Description 41
9.2 Flight Dynamics 41

REFERENCES 46

BIOGRAPHICAL SKETCH 49

LIST OF TABLES

Table page

6–1 Longitudinal eigenvectors 27

6–2 Longitudinal eigenvalues 28

6–3 Lateral-directional eigenvectors 28

6–4 Lateral-directional eigenvalues 28

6–5 Lateral-directional eigenvector 29

7–1 Gains for span varying disturbance rejection controller 35

8–1 Gains for camber varying disturbance rejection controller 40

9–1 Gains for chord varying disturbance rejection controller 45

LIST OF FIGURES

Figure page

2–1 LIG-7 5

2–2 ICE Aircraft 6

2–3 Boeing Dragonfly 7

2–4 Virginia Tech BetaMax 7

2–5 Wing Curling MAV 8

2–6 Multi Point Wing Shaping MAV 9

2–7 AVCAAF Morphing Aircraft 9

2–8 Variable Gull-Wing MAV 10

3–1 Earth and Body Reference Frames 12

6–1 Base Model 27

7–1 Morphing Span 31

7–2 Pitching Moment Variation 32

7–3 Short Period Damping Ratio Variation 32

7–4 Short Period Frequency Variation 32

7–5 Phugoid Damping Ratio Variation 33

7–6 Phugoid Frequency Variation 33

7–7 Pole Migration of Longitudinal Modes 34

7–8 Dutch Roll Damping Ratio Variation 34

7–9 Dutch Roll Frequency Variation 34

7–10 Pole Migration of Lateral Modes 35

7–11 Pitch Response for Morphing Span 35

8–1 Morphing Camber 36

8–2 Pitching Moment Variation 37

8–3 Short Period Damping Ratio Variation 37
8–4 Short Period Frequency Variation 38
8–5 Phugoid Damping Ratio Variation 38
8–6 Phugoid Frequency Variation 38
8–7 Pole Migration of Longitudinal Modes 39
8–8 Dutch Roll Damping Ratio Variation 39
8–9 Dutch Roll Frequency Variation 39
8–10 Pole Migration of Lateral Modes 40
8–11 Pitch Response for Morphing Camber 40
9–1 Morphing Chord 41
9–2 Pitching Moment Variation 42
9–3 Short Period Damping Ratio Variation 42
9–4 Short Period Frequency Variation 42
9–5 Phugoid Damping Ratio Variation 43
9–6 Phugoid Frequency Variation 43
9–7 Pole Migration of Longitudinal Modes 43
9–8 Dutch Roll Damping Ratio Variation 44
9–9 Dutch Roll Frequency Variation 44
9–10 Pole Migration of Lateral Modes 44
9–11 Pitch Response for Morphing Chord 45

NOMENCLATURE

Symbol	Meaning
H	angular momentum
t	time
$\bar{r}$	position vector
L	moment about the x axis
M	moment about the y axis
N	moment about the z axis
p	angular rate about the x axis
q	angular rate about the y axis
r	angular rate about the z axis
u	velocity in the x direction
v	velocity in the y direction
w	velocity in the z direction
ϕ	roll angle
θ	pitch angle
ψ	yaw angle
I	moment of inertia
m	mass
$\bar{v}$	velocity vector
$\bar{a}$	acceleration
$\bar{\omega}$	angular velocity vector
F	force
g	gravity

Abstract of Thesis Presented to the Graduate School
of the University of Florida in Partial Fulfillment of the
Requirements for the Degree of Master of Science

DYNAMIC MODELING AND FLIGHT CONTROL OF MORPHING AIR VEHICLES

By

Kenneth E. Boothe Jr.

December 2004

Chair: Richard C. Lind, Jr.
Major Department: Mechanical and Aerospace Engineering

The majority of airplanes in use today fly with a fixed shape and use conventional control effectors such as elevators, ailerons, rudder. These control surfaces are used in lieu of changing the entire shape of the airplane in an optimal manner because a global change in geometry includes far more complexity, and possibly an associated weight increase along with a decreased level of reliability. Advances in materials and new ideas in the area of structures are opening up possibilities to aircraft designers. These advances are ushering in morphing aircraft as a new class of air vehicle. This prospect is being pursued and several morphing air vehicles are already in various stages of development and flight testing. This emerging area of study is initiating a need for dynamic models and control strategies to work within its framework.

CHAPTER 1
INTRODUCTION

A flight vehicle is typically designed to function around a primary operating point. This design point may be an efficient cruise for a transport while a fighter may seek to optimize maneuverability and to increase top speed. Performance and efficiency begin to suffer as the airplane moves to other portions of the flight envelope. Advancements in materials science are offering the aerospace industry some unique and exciting possibilities for future aircraft configurations that will be able to address these ever present design trade-offs [14]. Emerging technologies such as embedded actuators and shape memory alloys are on the horizon and will benefit many engineering disciplines. The obvious aerospace application is to have an airplane that is capable of changing its shape to either adapt to various flight conditions or provide increased maneuverability [5]. This concept, known as morphing aircraft, presents some new and exciting challenges to the aerospace industry. There is ongoing research in the aerospace community dealing with the many issues in this inherently multi-disciplinary arena.

Micro air vehicles (MAVs), a small-sized class within the general class of unpiloted air vehicles (UAVs), are now more commonly coming under consideration for carrying out existing missions as well as those that can only be completed by a MAV. The dimensions of the aircraft coupled with its small mass afford it some unique capabilities along with significant advantages over larger, more expensive UAVs. A MAV can enter into and navigate through urban environments that a conventionally sized UAV can not. Materials and labor scale down along with the size, ensuring that the overall flyaway cost is lowered. The low mass and slow forward speed of a MAV both contribute to lowering the kinetic energy absorbed

by the airframe during a crash. Crashes are almost always survivable or easily repairable. An accident such as an actuator failure will most likely spell an end to a UAV at a considerable cost; however, the same incident may not even incur any damage on the inexpensive MAV.

These benefits are attracting attention from both military and civilian sectors. This interest is translating into challenging research opportunities for the aerospace community. One obstacle facing advancement in this area is that aerodynamics on this scale are not well solved at this point. Viscous forces begin to dominate in this Reynolds number regime and conventional inviscid analysis does not adequately solve for the flow field and resulting pressure distribution. There is also a hysteresis effect due to the unsteady boundary layer behavior during which it separates and then reattaches periodically [17]. Add to this already difficult subject by implementing morphing as a means of flight control and you present an even greater challenge. Now there exists a multidisciplinary design problem that lends itself to the coordination of several research teams. Aerodynamicists must coordinate their efforts with structural engineers to model the pressure distribution and design a wing to yield desired mode shapes. The dynamics of morphing micro air vehicles (MMAVs) must be solved before any sophisticated control theory can be applied.

Work is currently underway at the University of Florida to investigate the flight characteristics of a variety of MMAVs. Flight testing is a primary part of the design methodology [1]. Iterative design methods teach lessons on what works but not necessarily why it works. A common outcome of this procedure is first identifying a promising configuration and then going about trying to explain why it works well. A good example of this is the flexible wing concept. It was observed that MAVs with wings made of latex flew better than those with rigid wings. Then

a combinational approach was taken to solve for the aerodynamics as well as the structural dynamics [17].

System identification and parameter estimation can be arduous and expensive undertakings. Wind-tunnel testing can cost valuable man-hours and the accuracy of the data may be compromised by errors in calibration and implementation. Flight testing is a promising method with which to gather open-loop dynamic data. The problem with employing this technique on a MAV is the payload restrictions of a vehicle this size. The University of Florida MAV program has not yet advanced its flight testing program to the stage where full state feedback is achievable. Most importantly, the ability to measure angle of sideslip, angle of attack, and airspeed is not present. These modeling problems facing the MAV program lead naturally to the remaining option of analytical methods utilizing computational fluid dynamics (CFD).

The use of CFD independently of, or in concordance with, experimental data can expedite the generation of mathematical models [31]. An example of this cooperative modeling was done for the "active vision control for agile autonomous flight" vehicle (AVCAAF). A combination of static stability derivatives from wind tunnel testing and dynamic derivatives from *Tornado* was used to generate a full set of longitudinal and lateral dynamics for AVCAAF [13]. CFD is also useful in the preliminary design phases of new aircraft. This is the case of the three proposed morphing aircraft considered in this thesis. They have not been built and thusly can only be studied in terms of analytical methods.

The flight dynamics models of the MAVs here at the University of Florida have not fully matured. Design and analysis has always been driven by an iterative qualitative flight testing process. MAVs have also been controlled in large by a pilot in the loop and the limited amount of autopilot development has been achieved by a hand tuned PID type controller. An accurate mathematical model

must exist if the AVCAAF program is to advance the level of sophistication of controls research.

This thesis investigates the characterization of morphing aircraft and control laws to actively command the morphing. First the equations of motion are derived for an arbitrary morphing airplane. Small disturbance theory is used to linearize these equations. Then the equations are decoupled into seperate longitudinal and lateral models and written in terms of stability derivatives that can be estimated from CFD. CFD is then used to generate these longitudinal and lateral models for three different morphing aircraft. The three aircraft morph by changing their span, chord, and camber respectively. The models for these aircraft are generated as linear input varying (LIV) functions. This allows the use of new LIV control theories currently being developed at the University of Florida. Variations in characteristics including modal properties and flight dynamics of these models are examined and explained.

CHAPTER 2
MORPHING AIRCRAFT

2.1 History

The concept of morphing aircraft for flight control has been around as long as aircraft themselves and was implemented on the Wright Flyer in the form of wing warping. The Wright brothers observed birds and mimicked their wing twisting in order to facilitate roll control [6]. The use of morphing as a means of expanding the flight envelope also dates back to air history's early beginnings. A NACA report was released in 1920 detailing the "Parker Variable Camber Wing" [24]. The idea of this concept was to reduce the drag on the wing at higher speeds by changing the wing profile. Another early morphing pioneer was Razdviznoe Krylo from Russia. This company built the LIG-7 pictured in Figure 2–1 in 1932 which had an articulated surface that extracted to increase lift during take-off and landing while retracting for cruise [27].

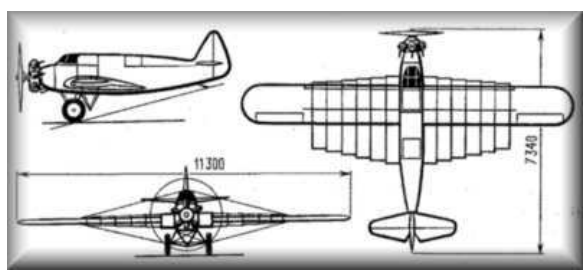

Figure 2–1: LIG-7

Morphing soon gave way to conventional control surfaces and flight vehicle configurations. Benefits of morphing mechanisms are often easily outweighed by drawbacks encountered during their implementation. Many devices such as shape memory alloys will provide an amazing bench top demonstration but are restricted in usage by the excess weight of the associated electronics. As material

science works to make morphing structures more usable, aerospace engineers should consider applications in anticipation of coming advancements [26, 7]. Such an example of this is the Lockheed Martin Tactical Aircraft Systems - Innovative Control Effectors (LMTAS-ICE) concept vehicle shown in Figure 2–2. This configuration is being considered to test the concept of novel control effectors in improving weight, cost, stealth, and performance [23, 25].

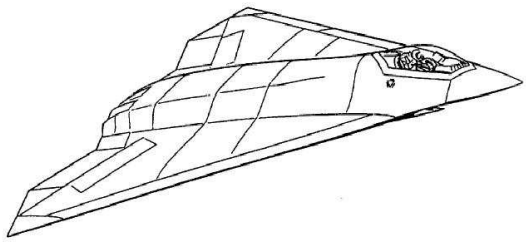

Figure 2–2: ICE Aircraft

There are a limited number of morphing aircraft that have been built and test flown. One of these is the Boeing Dragonfly UAV shown in Figure 2–3. This unique rotor-craft transitions from hovering to forward flight by stopping its rotor blades and fixing them so they can act as wings. The Dragonfly has been built and has demonstrated hovering flight. Virginia Tech has designed, built, and successfully flown a smaller morphing airplane called the BetaMax (Figure 2–4). This airplane uses the same concept as the one discussed later here in Chapter 5. Another point of relevance for the BetaMax is that they used the same CFD software as this thesis to estimate some aerodynamic coefficients and predict performance parameters like range.

2.2 University of Florida Micro Air Vehicles

A number of morphing micro air vehicles have been designed, flight tested, and studied at the University of Florida [18]. Primarily various types of wing warping have been used as a means of roll control to achieve greater agility, which is a crucial issue for MAVs [30, 29, 28]. Micro air vehicles have the ability to fly in

Figure 2–3: Boeing Dragonfly

Figure 2–4: Virginia Tech BetaMax

small spaces that a large airplane can not. A common scenario under consideration is maneuvering through an urban canyon environment. This concept requires that a MAV be able to enter into and navigate through a maze of buildings to carry out missions such as chemical detection or sensor emplacement [11].

Fig 2–5 shows a wing curling MAV. The wing is designed and built in such a way that it can be morphed by simply pulling a small Kevlar thread attached to

the wing panel. This novel control effector caused a significantly greater roll rate than the pre-existing conventional control surfaces [14].

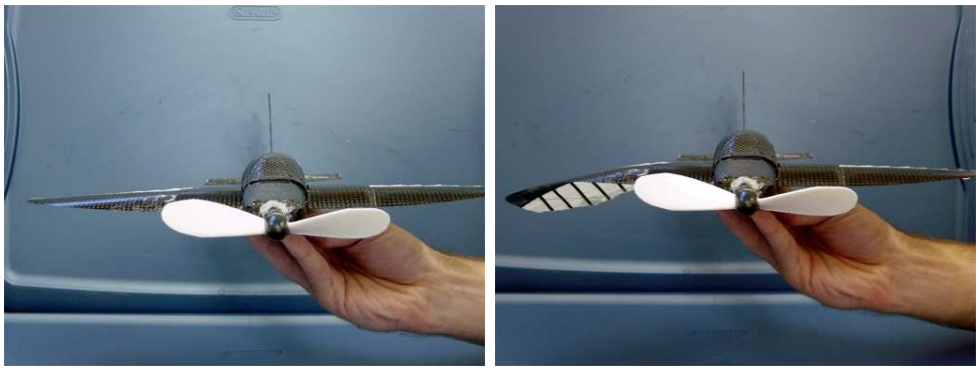

Figure 2–5: Wing Curling MAV

Fig 2–6 shows another example of a MAV using wing twist as control effector. This aircraft has a considerably more complicated morphing mechanism. The wing is articulated in two separate sections to facilitate the study of a variety of complex shapes. The goal is to have some measure of control over the wing lift distribution. The wing on this aircraft is being actuated both symmetrically to quasi-statically affect the spanwise lift distribution and asymmetrically for roll control.

The University of Florida's 'Active Vision for Control of Agile Autonomous Flight' vehicle (AVCAAF) uses a proprietary vision based autopilot being developed at the University of Florida to achieve three dimensional waypoint navigation [15], [16]. The AVCAAF flight vehicle seen in Fig 2–7 employs yet another variant of wing twisting. The AVCAAF has a adopted a simple mechanism that twists the wing at the root and globally morphs the rest of the wing. This vehicle s being developed for use by special forces and has the need to be somewhat more durable than a lot of the more experimental MAVs being produced by the University of Florida [12]. AVCAAF is still in the early testing phases, but it appears as though this form of wing morphing is superior to the previous conventional control surfaces in affecting roll control.

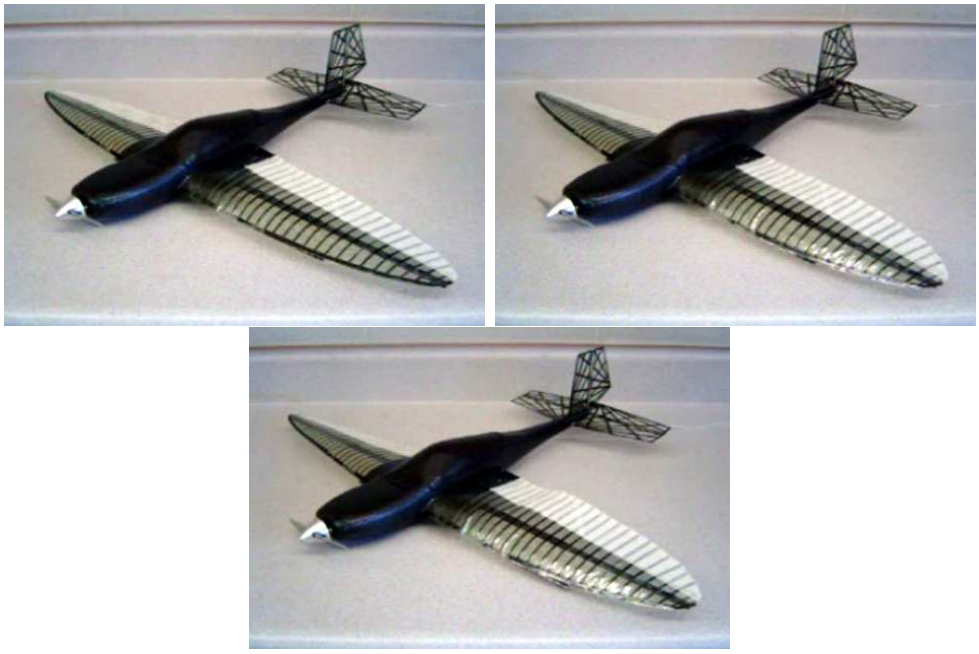

Figure 2–6: Multi Point Wing Shaping MAV

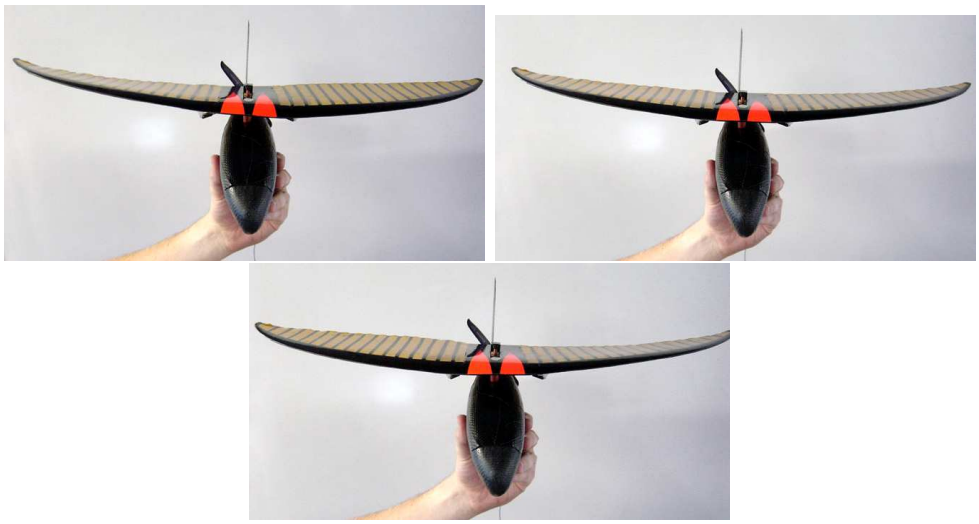

Figure 2–7: AVCAAF Morphing Aircraft

Fig 2–8 is a biologically inspired variable gull wing MAV that was developed to mimic different wing configurations used by birds in various phases of flight. The jack screw driven actuation system moves far to slowly too be used for flight path control. In turn it is used in a quasi-static manner to explore possibilities of flight envelope expansion and optimization. As the gull-wing angle is increased

in the positive direction, the vehicle becomes highly stable about the roll axis. Additionally, this morphing position diminishes the glide angle considerably, allowing the aircraft to descend at steep angles without increasing airspeed.

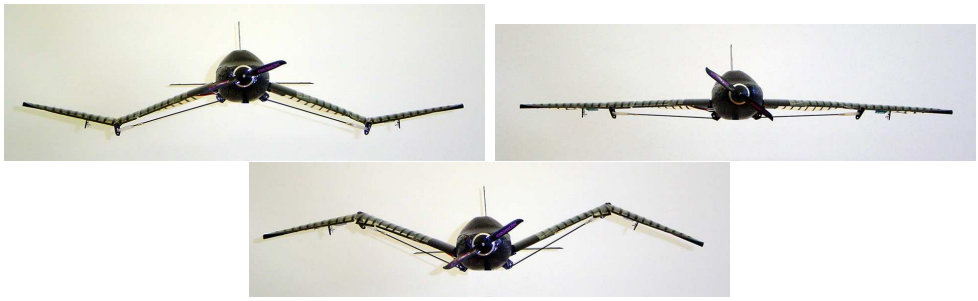

Figure 2–8: Variable Gull-Wing MAV

CHAPTER 3
MORPHING AIRCRAFT EQUATIONS OF MOTION

The equations of motion for morphing aircraft must be derived to describe maneuvering as the geometry changes. A simulation also needs to be created in order to study openloop responses and to test control laws. The framework for formulating vehicle dynamics from stability derivatives of a standard airplane differs from that of a morphing airplane. Morphing structures require additional considerations. The plant's functional dependence and the absence of a control matrix, as in the case of dynamic morphing, must be taken into account.

3.1 Nonlinear Equations of Motion

Below a derivation of the equations of motion (EOM) for an arbitrary morphing aircraft is performed. This is done in order to re-examine the assumptions typically made for a conventional aircraft of a fixed geometry. Terms that normally drop out during the reduction of the equations due to the configuration of a conventional airplane must be left intact to describe the dynamics of an arbitrary morphing aircraft. A set of EOM are derived by analyzing Newton's laws, as documented in textbooks [21] [32], but also incorporating terms that acount for time varying shape. The B and E coordinate frames referenced during the derivations are described in Fig 3–1

3.1.1 Angular Momentum

The aircraft moments are derived by setting the angular momentum equal to the applied moments as in Eq 3.1

$$\frac{d\bar{H}}{dt} = \bar{M} \tag{3.1}$$

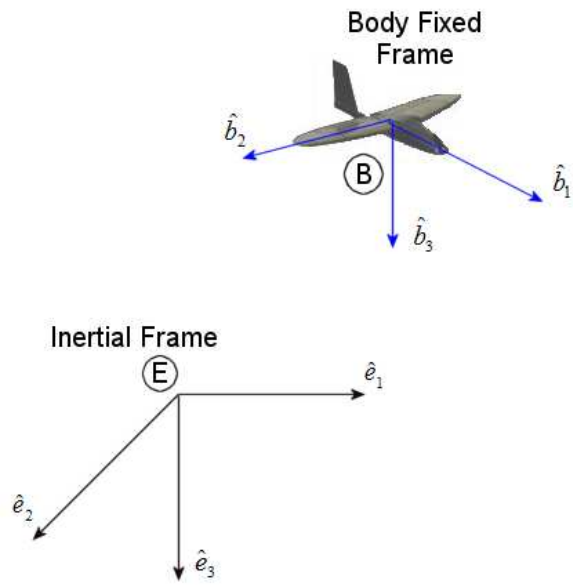

Figure 3–1: Earth and Body Reference Frames

where

$$\bar{H} = \bar{r} \times (m\bar{V}) \tag{3.2}$$

Eq 3.2 can be broken down further into three equations representing the individual moments (L, M, N).

$$L = \dot{H}_X + qH_Z - rH_Y \tag{3.3}$$

$$M = \dot{H}_Y + rH_X - pH_Z \tag{3.4}$$

$$N = \dot{H}_Z + pH_Y - qH_X \tag{3.5}$$

Eqs 3.6, 3.7, and 3.8 are the scalar equations for the moment of momentum.

$$H_X = pI_X - qI_{XY} - rI_{XZ} \tag{3.6}$$

$$H_Y = -pI_{XY} + qI_Y - rI_{YZ} \tag{3.7}$$

$$H_Z = -pI_{XZ} - qI_{YZ} + rI_Z \tag{3.8}$$

Substituting eqs 3.6, 3.7, and 3.8 into eqs 3.29, 3.30, and 3.31 gives the moment equations, eqs 3.3, 3.4, and 3.5.

$$L = \dot{p}I_X + p\dot{I}_X - \dot{q}I_{XY} - q\dot{I}_{XY} - \dot{r}I_{XZ} - r\dot{I}_{XZ} - qpI_{XZ} - q^2I_{YZ} + qrI_Z + rpI_{XY} - rqI_Y + r^2I_{YZ} \tag{3.9}$$

$$M = -\dot{p}I_{XY} - p\dot{I}_{XY} + \dot{q}I_Y + q\dot{I}_Y - \dot{r}I_{YZ} - r\dot{I}_{YZ} + rpI_X - rqI_{XY} - r^2I_{XZ} + p^2I_{XZ} + pqI_{YZ} - prI_Z \tag{3.10}$$

$$N = -\dot{p}I_{XZ} - p\dot{I}_{XZ} - \dot{q}I_{YZ} - q\dot{I}_{YZ} + \dot{r}I_Z + r\dot{I}_Z - p^2I_{XY} + pqI_Y - prI_{YZ} - qpI_X + q^2I_{XY} + qrI_{XZ} \tag{3.11}$$

These morphing EOM are left with some unique terms. These terms include all of the time variant moments of inertia $\dot{I}$ and the products of inertia I_{YZ} and I_{XY} which are left to account for possible assymitries about the XZ plane.

3.1.2 Force Equations

The derivation of the three aircraft force equations is carried out by implementing Newtons 2nd law given in eq 3.12.

$$\frac{d(m\bar{V})}{dt} = \bar{F} \tag{3.12}$$

The assumption that the earth is an inertial reference frame is made due to the fact that rotation rate of the earth is much slower than the angular rates of the aircraft. Another assumption is that the aircraft is a rigid body. The equations are usually expressed in the body coordinate frame (B) and mapped into the earth frame (E) by the Euler angles (ϕ, θ, ψ). Noting that Eq 3.12 is essentially $F = m\bar{a}$, Eq 3.13 can be used to compute the acceleration of the B frame in the E frame.

$$\bar{a}_E = \dot{\bar{v}}_B + \bar{\omega}_B \times \bar{v}_B \tag{3.13}$$

The velocity is v_B is given by Eq 3.14

$$\bar{v} = u\hat{i} + v\hat{j} + w\hat{k} \tag{3.14}$$

where u,v, and w are the velocities in the x, y, and z body axes and the rate of rotation of the body frame in the inertial frame is given by Eq 3.15

$$\bar{\omega}_B = p\hat{i} + q\hat{j} + r\hat{k} \tag{3.15}$$

Multiplying by the mass of the aircraft and separating the vector equation into the three force equations yields Eqs 3.16, 3.17, and 3.18,

$$m(\dot{u} + qw - rv) = F_x, \tag{3.16}$$

$$m(\dot{v} + ru - pw) = F_y, \tag{3.17}$$

$$m(\dot{w} + pv - qu) = F_z, \tag{3.18}$$

F_x, F_y, and F_z can be separated into gravitational (mg) and propulsive forces (X, Y, Z). Performing this separation and applying a rotation transformation leads to Eqs 3.19, 3.20, and 3.21.

$$X - mgS_\theta = m(\dot{u} + qw - rv) \tag{3.19}$$

$$Y + mgC_\theta S_\phi = m(\dot{v} + ru - pw) \tag{3.20}$$

$$Z + mgC_\theta C_\phi = m(\dot{w} + pv - qu) \tag{3.21}$$

3.1.3 Attitude and Angular Velocities

The relationship between the angular velocities (p, q, r) in the body frame and the Euler rates ($\dot{\psi}, \dot{\theta}$, and $\dot{\phi}$) are obtained by applying a sequence of rotations to the aircraft and are given by Eqs 3.22, 3.23, and 3.24

$$p = \dot{\phi} - \dot{\psi}S_\theta \tag{3.22}$$

$$q = \dot{\theta}C_\phi + \dot{\psi}C_\theta S_\psi \tag{3.23}$$

$$r = \dot{\psi}C_\theta C_\phi - \dot{\theta}S_\phi \tag{3.24}$$

$$\dot{\theta} = qC_\phi - rS_\phi \tag{3.25}$$

$$\dot{\phi} = p + qS_\phi T_\theta + rC_\phi T_\theta \tag{3.26}$$

$$\dot{\psi} = (qS_\phi + rC_\phi) sec\ \theta \tag{3.27}$$

3.2 Linearized Equations of Motion

Small disturbance theory is used to linearize the EOMs about an operating condition. This is done by replacing all of the variables in the equations of motion by a reference value plus a disturbance.

3.2.1 Angular Momentum

Substituting the equations in 3.28 into Eqs 3.9, 3.10, and 3.11

$$\begin{aligned} p &= p_0 + \Delta p & \dot{p} &= \Delta\dot{p} \\ q &= q_0 + \Delta q & \dot{q} &= \Delta\dot{q} \\ r &= r_0 + \Delta r & \dot{r} &= \Delta\dot{r} \end{aligned} \tag{3.28}$$

yields Eqs 3.9, 3.10, and 3.11

$$\begin{aligned} L =& \Delta\dot{p}I_X + (p_0 + \Delta p)\dot{I}_X - \Delta\ \dot{q}I_{XY} - (q_0 + \Delta q)\dot{I}_{XY} - \Delta\dot{r}I_{XZ} - (r_0\Delta r)\dot{I}_{XZ} - \\ & (q_0p_0\Delta qp_0 + \Delta pq_0\Delta p\Delta q)I_{XZ} - (q_0^2 + 2\Delta qq_0 + \Delta q^2)I_{YZ} + \\ & (q_0r_0 + \Delta qr_0\Delta rq_0 + \Delta r\Delta q)I_Z + (r_0p_0 + \Delta rp_0 + \Delta pr_0\Delta r\Delta p)I_{XY} - \\ & (r_0q_0 + \Delta rq_0 + \Delta qr_0\Delta r\Delta q)I_Y + (r_0^2 + 2\Delta rr_0 + \Delta r^2)I_{YZ} \end{aligned} \tag{3.29}$$

$$
\begin{aligned}
M = &- \Delta\dot{p}I_{XY} - (p_0 + \Delta p)\dot{I}_{XY} + \Delta\dot{q}I_Y + (q_0 + \Delta q)\dot{I}_Y - \Delta\dot{r}\dot{I}_{YZ} - (r_0 + \Delta r)\dot{I}_{YZ} + \\
&(r_0 p_0 + \Delta r p_0 + \Delta p r_0)I_X - (r_0 q_0 \Delta r q_0 + \Delta q r_0)I_{XY} + (r_0^2 + 2\Delta r r_0)I_{XZ} - \\
&(p_0^2 + 2\Delta p p_0)I_{XZ} + (r_0^2 + 2\Delta r r_0 + \Delta r^2)I_{YZ}
\end{aligned}
\tag{3.30}
$$

$$
\begin{aligned}
N = &\Delta\dot{p}I_X + (p_0 + \Delta p)\dot{I}_X - \Delta\dot{q}I_{XY} - (q_0 + \Delta q)\dot{I}_{XY} - \Delta\dot{r}I_{XZ} - (r_0\Delta r)\dot{I}_{XZ} - \\
&(q_0 p_0 \Delta q p_0 + \Delta p q_0 \Delta p \Delta q)I_{XZ} - (q_0^2 + 2\Delta q q_0 + \Delta q^2)I_{YZ} + \\
&(q_0 r_0 + \Delta q r_0 \Delta r q_0 + \Delta r \Delta q)I_Z + (r_0 p_0 + \Delta r p_0 + \Delta p r_0 \Delta r \Delta p)I_{XY} - \\
&(r_0 q_0 + \Delta r q_0 + \Delta q r_0 \Delta r \Delta q)I_Y + (r_0^2 + 2\Delta r r_0 + \Delta r^2)I_{YZ}
\end{aligned}
\tag{3.31}
$$

simplifying

$$
\begin{aligned}
L = &\Delta\dot{p}I_X - \Delta\dot{q}I_{XY} - \Delta\dot{r}I_{XZ} + \Delta p(\dot{I}_X - q_0 I_{XZ} + r_0 I_{XY}) + \\
&\Delta q(-\dot{I}_{XY} - p_0 I_{XZ} - 2q_0 I_{YZ} + r_0 I_Z - r_0 I_Y) + \\
&\Delta r(-\dot{I}_{XZ} + q_0 I_Z + p_0 I_{XY} - q_0 I_Y + 2r_0 I_{YZ}) + \\
&p_0\dot{I}_X - q_0\dot{I}_{XY} - r_0\dot{I}_{XZ} - q_0^2 I_{YZ} + q_0 r_0 I_Z + r_0 p_0 I_{XY} - r_0 q_0 I_y + r_0^2 I_{YZ}
\end{aligned}
\tag{3.32}
$$

$$
\begin{aligned}
M = &\Delta\dot{p}I_x - \Delta\dot{q}I_{XY} - \Delta\dot{r}I_{XZ} + \Delta p(\dot{I}_X - q_0 I_{XZ} + r_0 I_{XY}) + \\
&\Delta q(-\dot{I}_{XY} - p_0 I_{XZ} - 2q_0 I_{YZ} + r_0 I_Z - r_0 I_Y) + \\
&\Delta r(-\dot{I}_{XZ} + q_0 I_Z + p_0 I_{XY} - q_0 I_Y + 2r_0 I_{YZ}) + \\
&p_0\dot{I}_X - q_0\dot{I}_{XY} - r_0\dot{I}_{XZ} - q_0^2 I_{YZ} + q_0 r_0 I_Z + r_0 p_0 I_{XY} - r_0 q_0 I_y + r_0^2 I_{YZ}
\end{aligned}
\tag{3.33}
$$

$$
\begin{aligned}
N =& \Delta\dot{p}I_{XZ} - \Delta\dot{q}I_{XY} - \Delta\dot{r}I_{XZ} + \Delta p(\dot{I}_X - q_0 I_{XZ} + r_0 I_{XY}) + \\
& \Delta q(-\dot{I}_{XY} - p_0 I_{XZ} - 2q_0 I_{YZ} + r_0 I_Z - r_0 I_Y) + \\
& \Delta r(-\dot{I}_{XZ} + q_0 I_Z + p_0 I_{XY} - q_0 I_Y + 2r_0 I_{YZ}) + \\
& p_0\dot{I}_X - q_0\dot{I}_{XY} - r_0\dot{I}_{XZ} - q_0^2 I_{YZ} + q_0 r_0 I_Z + r_0 p_0 I_{XY} - r_0 q_0 I_y + r_0^2 I_{YZ}
\end{aligned}
\tag{3.34}
$$

3.2.2 Force Equations

Now the force equations are linearized by the same method, substituting the values from 3.42 into Eqs 3.19, 3.20, and 3.21

$$
\begin{aligned}
X &= X_0 + \Delta X & \dot{X} &= \Delta\dot{X} \\
Y &= Y_0 + \Delta Y & \dot{Y} &= \Delta\dot{Y} \\
Z &= Z_0 + \Delta Z & \dot{Z} &= \Delta\dot{Z} \\
u &= u_0 + \Delta u & \dot{u} &= \Delta\dot{u} \\
v &= v_0 + \Delta v & \dot{v} &= \Delta\dot{v} \\
w &= w_0 + \Delta w & \dot{w} &= \Delta\dot{w}
\end{aligned}
\tag{3.35}
$$

$$
X_0 + \Delta X - mg\ sin(\theta_0 + \Delta\theta) = m[\Delta\dot{u} + (q_0 + \Delta q)(w_0 + \Delta w) - (r_0 + \Delta r)(v_0 + \Delta v)]
\tag{3.36}
$$

$$
Y_0 + \Delta Y - mg\ cos(\theta_0 + \Delta\theta)\ sin(\phi_0 + \Delta\phi) = m[\Delta\dot{v} + (r_0 + \Delta r)(u_0 + \Delta u) - (p_0 + \Delta p)(w_0 + \Delta w)]
\tag{3.37}
$$

$$
Z_0 + \Delta Z - mg\ cos(\theta_0 + \Delta\theta)\ cos(\phi_0 + \Delta\phi) = m[\Delta\dot{w} + (p_0 + \Delta p)(v_0 + \Delta v) - (q_0 + \Delta q)(u_0 + \Delta u)]
\tag{3.38}
$$

Expanding

$$X_0 + \Delta X - mg\ sin(\theta_0 + \Delta\theta) = m[\Delta\dot{u} + (q_0 w_0 + \Delta q w_0 + \Delta w q_0) - (r_0 v_0 + \Delta r v_0 + \Delta v r_0)] \tag{3.39}$$

$$Y_0 + \Delta Y - mg\ cos(\theta_0 + \Delta\theta)\ sin(\phi_0 + \Delta\phi) = m[\Delta\dot{v} + (r_0 u_0 + \Delta r u_0 + \Delta u r_0) - (p_0 w_0 + \Delta p w_0 + \Delta w p_0)] \tag{3.40}$$

$$Z_0 + \Delta Z - mg\ cos(\theta_0 + \Delta\theta)\ cos(\phi_0 + \Delta\phi) = m[\Delta\dot{w} + (p_0 v_0 + \Delta p v_0 + \Delta v p_0) - (q_0 u_0 + \Delta q u_0 + \Delta u q_0)] \tag{3.41}$$

3.2.3 Attitude and Angular Velocities

The same procedure is repeated for the attitude and angular velocity equations. Substituting the values in 3.42 into eqs 3.22, 3.23, and 3.24

$$\begin{aligned} p &= p_0 + \Delta p & \dot{p} &= \Delta\dot{p} \\ q &= q_0 + \Delta q & \dot{q} &= \Delta\dot{q} \\ r &= r_0 + \Delta r & \dot{r} &= \Delta\dot{r} \\ \phi &= \phi_0 + \Delta\phi & \dot{\phi} &= \Delta\dot{\phi} \\ \psi &= \psi_0 + \Delta\psi & \dot{\psi} &= \Delta\dot{\psi} \\ \theta &= \theta_0 + \Delta\theta & \dot{\theta} &= \Delta\dot{\theta} \end{aligned} \tag{3.42}$$

gives

$$p_0 + \Delta p = \Delta\dot{\phi} - \Delta\dot{\psi} sin(\theta_0 + \Delta\theta) \tag{3.43}$$

$$q_0 + \Delta q = \dot{\theta} cos(\Delta\phi + \phi_0) + \Delta\dot{\psi} cos(\theta_0 \Delta\theta) sin(\psi_0 + \Delta\psi) \tag{3.44}$$

$$r_0 + \Delta r = \Delta\dot{\psi} cos(\theta_0 \Delta\theta) cos(\phi_0 \Delta\phi) - \Delta\dot{\theta} sin(\phi_0 + \Delta\phi) \tag{3.45}$$

$$\Delta\dot{\theta} = (q_0 + \Delta q) cos(\phi_0 + \Delta\phi) - (r_0 + \Delta r) sin(\phi_0 + \Delta\phi) \tag{3.46}$$

$$\begin{aligned} \Delta\dot{\phi} =& (p_0 + \Delta p) + (q_0 + \Delta q) sin(\phi_0 + \Delta\phi) tan(\theta_0 + \Delta\theta) + \\ & (r_0 + \Delta r) cos(\phi_0 + \Delta\phi) tan(\theta_0 + \Delta\theta) \end{aligned} \tag{3.47}$$

$$\Delta\dot{\psi} = (q_o + \Delta q) sin(\phi_0 + \Delta\phi) + (r_0 + \Delta r) cos(phi_0 + \Delta\phi) sec(\theta_0 + \Delta\theta) \tag{3.48}$$

3.3 Straight and Level Flight

Next equations are written to describe straight and level flight. Take the X force equation, eq 3.39, as an example to explain the process. Straight and level is described by assuming symetric flight. This implies that $w_0 = v_0 = p_0 = q_0 = r_0 = \Phi_0 = \psi_0 = 0$. Applying this assumption to eq 3.39 produces eq 3.49.

$$X_0 + \Delta X - mg\ sin(\theta_0 + \Delta\theta) = m\Delta\dot{u} \tag{3.49}$$

Eq 3.49 can be further reduced with the use of the trigonemetric identity in Eq 3.50.

$$sin(\theta_o + \Delta\theta) = sin\ \theta_0\ cos\ \Delta\theta + cos\ \theta_0\ sin\ \Delta\theta = sin\ \theta_0 + \Delta\theta\ cos\ \theta_0 \tag{3.50}$$

Plugging Eq 3.50 into Eq 3.49 yields Eq 3.51.

$$X_0 + \Delta X - mg(sin\ \theta_0 + \Delta\theta\ cos\ \theta_0) = m\Delta\dot{u} \tag{3.51}$$

Individual Taylor series expansions are used to express the aerodynamic forces and moments on the airplane. These expansions are done as a perturbations about the reference flight conditions under the assumtion that the perturbations are all

instananeous changes from the filght conditions. The expansions are done with consideration to their dependant variables. The choice of dependant variables is made to insure decoupling of the aircraft dynamics into a set of longitudunal equations and a set of lateral equations. The example using the X force equation is continued as follows.

Setting all of disturbances equal to zero gives Eq 3.52, the reference flight condition.

$$X_0 - mgsin\ \theta_0 = 0 \tag{3.52}$$

This reduces the X force equation to Eq 3.53.

$$\Delta X - mg\Delta\theta\ cos\ \theta_0 = m\Delta\dot{u} \tag{3.53}$$

Decoupling requires that the dependant variables be chosen to reflect changes strictly in either the longitudinal or lateral sense. X is a longitudinal force so it is assumed that $X = f(u, w, \Delta\delta_e, \Delta\delta_T)$ where δ_e and δ_T are the changes in elevator deflection and thrust, resptectively. The expansion of ΔX in Eq 3.53 is carried out in Eq 3.54

$$\Delta X = \frac{\delta X}{\delta u}\Delta u + \frac{\delta X}{\delta w}\Delta w + \frac{\delta X}{\delta\delta_e}\Delta\delta_e + \frac{\delta X}{\delta\delta_T}\Delta\delta_T \tag{3.54}$$

Eq 3.54 is substituted into Eq 3.53 to yield Eq 3.55

$$\frac{\delta X}{\delta u}\Delta u + \frac{\delta X}{\delta w}\Delta w + \frac{\delta X}{\delta\delta_e}\Delta\delta_e + \frac{\delta X}{\delta\delta_T}\Delta\delta_T - mg\Delta\theta\ cos\ \theta_0 = m\Delta\dot{u} \tag{3.55}$$

Dividing Eq 3.55 through by the mass m and defining the format for the aerodynamic derivatives as $X_u = \delta X/\delta u/m$, $X_w = \delta X/\delta w/m$, and so on allows for Eq 3.55 to be written as Eq 3.56

$$(\frac{d}{dt} - X_u)\Delta u - X_w \Delta w + (g\ cos\theta_0)\Delta\theta = X_{\delta_e}\Delta\delta_e + X_{\delta_T}\Delta\delta_T \tag{3.56}$$

The remaining two force equations along with the three moment equations are treated in a similar manner and then placed into the state space form and given in Eqs 3.57, and 3.58.

Longitudinal state space:

$$\begin{bmatrix} \Delta\dot{u} \\ \Delta\dot{w} \\ \Delta\dot{q} \\ \Delta\dot{\theta} \end{bmatrix} = \begin{bmatrix} X_u & X_w & 0 & -g \\ Z_u & Z_w & u_0 & 0 \\ M_u + M_{\dot{w}}Z_u & M_w + M_{\dot{w}}Z_w & M_q + M_{\dot{w}}u_0 & 0 \\ 0 & 0 & 1 & 0 \end{bmatrix} \begin{bmatrix} \Delta u \\ \Delta w \\ \Delta q \\ \Delta\theta \end{bmatrix} \tag{3.57}$$

Lateral state space:

$$\begin{bmatrix} \Delta\dot{\beta} \\ \Delta\dot{p} \\ \Delta\dot{r} \\ \Delta\dot{\phi} \end{bmatrix} = \begin{bmatrix} \frac{Y_\beta}{u_0} & \frac{Y_p}{u_0} & -(1 - \frac{Y_r}{u_0}) & \frac{g\cos\theta_0}{u_o} \\ L_\beta & L_p & L_r & 0 \\ N_\beta & N_p & N_r & 0 \\ 0 & 1 & 0 & 0 \end{bmatrix} \begin{bmatrix} \Delta\beta \\ \Delta p \\ \Delta r \\ \Delta\phi \end{bmatrix} \tag{3.58}$$

CHAPTER 4
MODELING

Now $\dot{X} = AX$ becomes $\dot{X} = A(\mu)X$ where $A(\mu) = A_N\mu^N + A_{N-1}\mu^{N-1} + A_{N-2}\mu^{N-2} + ...A_2\mu^2 + A_1\mu + A_0$. If $N = 1$ i.e. $\dot{X} = (A_1\mu + A_0)X$ then the system falls into the class of LIV systems.

In the case of morphing aircraft, the dynamics are dependent on a varying parameter of the changing geometry. In order to characterize the dynamics over the range of actuation, models must be created at various points in the parameter space. These models are then curve fit against the varying parameter using the least squares method. Now $A = f(\mu)$ where μ is the morphing parameter. The dynamics are then represented by $\dot{X} = A(\mu)X$ where $A(\mu) = A_N\mu^N + A_{N-1}\mu^{N-1} + A_{N-2}\mu^{N-2} + ...A_2\mu^2 + A_1\mu + A_0$. If $N = 1$ i.e. $\dot{X} = (A_1\mu + A_0)X$ then the system falls into the class of linear input varying (LIV) systems. N can be chosen such that the order of the function f properly identifies the relationship between the varying parameter and the dynamics. This curve fit can be done for any order of polynomial. Now the dynamics are represented by:

Longitudinal states:

$$\begin{bmatrix} \Delta\dot{u} \\ \Delta\dot{w} \\ \Delta\dot{q} \\ \Delta\dot{\theta} \end{bmatrix} = \begin{bmatrix} X_u(\mu) & X_w(\mu) & 0 & -g \\ Z_u(\mu) & Z_w(\mu) & u_0 & 0 \\ M_u(\mu) + M_{\dot{w}}(\mu)Z_u(\mu) & M_w(\mu) + M_{\dot{w}}(\mu)Z_w(\mu) & M_q(\mu) + M_{\dot{w}}(\mu)u_0 & 0 \\ 0 & 0 & 1 & 0 \end{bmatrix} \begin{bmatrix} \Delta u \\ \Delta w \\ \Delta q \\ \Delta\theta \end{bmatrix} \tag{4.1}$$

Lateral states:

$$\begin{bmatrix} \Delta\dot{\beta} \\ \Delta\dot{p} \\ \Delta\dot{r} \\ \Delta\dot{\phi} \end{bmatrix} = \begin{bmatrix} \frac{Y_\beta(\mu)}{u_0} & \frac{Y_p(\mu)}{u_0} & -(1-\frac{Y_r(\mu)}{u_0}) & \frac{g\cos\theta_0}{u_o} \\ L_\beta(\mu) & L_p(\mu) & L_r(\mu) & 0 \\ N_\beta(\mu) & N_p(\mu) & N_r(\mu) & 0 \\ 0 & 1 & 0 & 0 \end{bmatrix} \begin{bmatrix} \Delta\beta \\ \Delta p \\ \Delta r \\ \Delta\phi \end{bmatrix} \tag{4.2}$$

CHAPTER 5
CONTROL SYNTHESIS

5.1 Quasi-static Morphing

Morphing has two distinct possible implementations; dynamic and quasi-static. Dynamic morphing involves the use of variable geometry as a control effector. Quasi-static morphing employs shape changes to optimize performance over the flight envelope. In this architecture conventional control surfaces are used for control and morphing is used only to reconfigure the aircraft to shapes optimized for different portions of the flight envelope. This allows for the application of existing control strategies. One method of controlling this type of vehicle is to design an optimal controller for a set of dynamics in the middle of the parameter space. The intent is to obtain a set of controller gains that retain stability with a slight degradation in performance metrics.

5.2 Dynamic Morphing

Sufficient actuator dynamics can allow for dynamic morphing. This concept involves a change in geometry that is both fast and extensive enough to enable flight path control with sufficient maneuverability. This type of plant falls into the class of LIV systems. LIV systems are an emerging class of systems whose dynamics are not only subject to change with operating parameters but undergo a significant change due to input parameters as well. In this case the morphing parameter μ is the input parameter. Aircraft dynamics typically vary with exogenous inputs such as altitude and mach number. There are existing control methodologies that deal with these variations, with gain scheduling being the most common approach. This procedure can be extended as in the case of the linear parameter varying (LPV) framework. LIV systems present a new challenge to the control theorist because

there is no control matrix in the traditional sense. Now proofs are given for the two Lemmas used in control design for the following apllications.

The controller design is given by the following Lemmas in [4]. These Lemmas were developed using a Lyapunov based method [19].

Lemma 1 *Given the system,* $\dot{x} = (A_0 + A_1 u)x$, *then the origin is globally asymptotically stable using the control law* $u = Kx$ *if*

1. $0 > A_0$
2. $0 > A_1 K$

Proof *The closed loop system is*

$\dot{x} = (A_0 + A_1 u)x$

where $\dot{x} = (A_0 + A_1(Kx))x$

$\dot{x} = A_0 + A_1(Kx)x \qquad K_1 \epsilon \mathcal{R}^{1xn},\ x \epsilon \mathcal{R}^{1xn},\ and\ u \epsilon \mathcal{R}$

$V(0) = 0$

$V(X) = x^T x > 0$

$\dot{V}(x) = \dot{x}^T x + x^T \dot{x}$

$$\begin{aligned}\dot{V}(x) &= [A_0 x + A_1(Kx)x]^T x + X^T[A_0 x + A_1(Kx)x] \\ &= x^T[(A_0 + A_1 K_0)x + A_1(K_1 x^2)]^T x + x^T[(A_0 + A_1 K_0) + A_1(K_1 x^2)]x \\ &= x^T A_0^T x + X^T A_1^T(Kx)x + x^T A_0 x + x^T A_1^T(Kx)xK_0) + A_1(K_1 x^2)]]x\end{aligned}$$

i.e. if the V *is negative definite*

$V(x) < 0\ if$

$A_0^T < 0$

$A_1^T(Kx) < 0$

$A_0 < 0$

$A_1(Kx) < 0 \qquad \forall\ x$

Lemma 2 *Given the system,* $\dot{x} = (A_0 + A_1 u)x$, *then the origin is globally asymptotically stable using the control law* $u = K_0 + K_1 x^2$ *if*

1. $0 > A_0$
2. $0 > A_1 K_2$

Proof *The closed loop system is*

$\dot{x} = (A_0 + A_1 u)x$

where $\dot{x} = (A_0 + A_1(K_0 + K_1 x^2))x$

$\dot{x} = (A_0 + A_1 K_0)x + A_1 K_1 x^2 x \qquad K_1 \epsilon \mathcal{R}^{1xn}$

$V(0) = 0$

$V(X) = x^T x > 0$

$\dot{V}(x) = \dot{x}^T x + x^T \dot{x}$

$$\begin{aligned}\dot{V}(x) &= [(A_0 + A_1 K_0)x + A_1(K_1 x^2)x]^T x + X^T[(A_0 + A_1 K_0)x + A_1(K_1 x^2)x] \\ &= x^T[(A_0 + A_1 K_0)x + A_1(K_1 x^2)]^T x + x^T[(A_0 + A_1 K_0) + A_1(K_1 x^2)]x \\ &= x^T[[(A_0 + A_1 K_0)x + A_1(K_1 x^2)]^T + [(A_0 + A_1 K_0) + A_1(K_1 x^2)]]x\end{aligned}$$

$V(x) < 0 \; if$

$[(A_0 + A_1 K_0)x + A_1(K_1 x^2)]^T + [(A_0 + A_1 K_0) + A_1(K_1 x^2)] < 0$

i.e. if the V *is negative definite*

Expanding $\dot{V}(x)$

$\dot{V}(x) = x^T(A_0 + A_1 K_o)^T x + x^T(A_1(K_1 x^2))^T x + x^T(A_0 + A_1 K_o) + x^T A_1(K_1 x^2)x$

$(A_0 + A_1 K_0)^T < 0$

$(A_1(K_1 x^2))^T < 0$

$(A_0 + A_1 K_0) < 0$

$(A_1(K_1 x^2)) < 0 \qquad \forall\, x$

CHAPTER 6
APPLICATION - BASE MODEL

6.1 Vehicle Description

The morphing aircraft discussed in the next three chapters all share the same base model. It is therefore useful to examine the flight dynamics of this model and to identify the characteristic modes. This forms a basis for understanding the propagation of these modes as the model is morphed in various manners. A representation of this airplane can be seen in Fig 6–1.

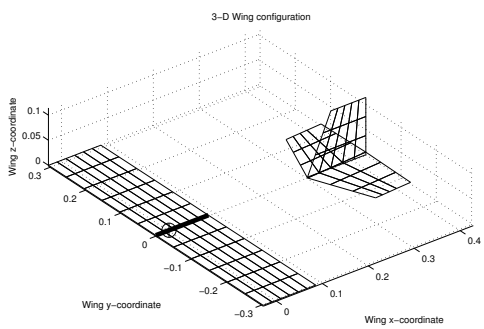

Figure 6–1: Base Model

The longitudinal eigenvectors are given in polar form in Table 6–1. These help to establish the phugoid and short period modes. The short period mode is dominated by w and q and the phugoid mode is characterized by a dominance of u and θ.

	Short Period Mode		Phugoid Mode	
	Magnitude	Phase	Magnitude	Phase
$\Delta\hat{u}$	0.5558	31.8695^o	11.3367	-92.9645^o
$\Delta\hat{w}$	16.7545	16.0589^o	0.5806	-87.8396^o
$\Delta\hat{q}$	17.1130	147.6617^o	0.8642	90.4741^o
$\Delta\theta$	1.0000	0.00^o	1.0000	0.00^o

Table 6–1: Longitudinal eigenvectors

Table 6–2 lists the modal properties of the longitudinal dynamics of the base model. Notice that the phugoid mode is very lightly damped and that the short period has a relatively high natural frequency.

Mode	Frequency (rad/s)	Damping
phugoid	0.8642	0.0083
short period	17.1130	0.8449

Table 6–2: Longitudinal eigenvalues

The lateral directional eigenvectors appear in Table 6–3. The roll mode can be identified by the dominance of ϕ and p. The unstable mode is recognized to be a spiral divergence. The eigenvector indicates the response resembles a classic spiral mode in that excitation of this mode is essentially yaw and roll.

	Roll Mode		Spiral Mode	
	Magnitude	Phase	Magnitude	Phase
$\Delta\hat{v}$	0.0619	180°	0.0849	0°
$\Delta\hat{p}$	14.5173	180°	0.6284	0°
$\Delta\hat{r}$	0.4423	0°	1.6893	0°
$\Delta\phi$	1.0000	0°	0.3720	0°
$\Delta\psi$	0.0305	180°	1.0000	0°

Table 6–3: Lateral-directional eigenvectors

Table 6–4 displays the modal properties of the lateral directional dynamics. The dutch roll frequency is reasonable for an aircraft of this size. The roll frequency seems rather high, but this aircraft was modeled with a thin carbon fiber wing and has an unusually low value for I_{xx} relative to the mass of the airplane.

Mode	Frequency (rad/s)	Damping
spiral	1.6893	1.0000
dutch roll	4.9812	0.6330
roll	14.5173	1.0000

Table 6–4: Lateral-directional eigenvalues

The stable mode has obvious characteristics associated with the classical definition of roll mode. The response of this mode is predominately a roll motion with only minor variation in angle of sideslip or yaw.

The remaining mode relates to a dutch roll dynamics as evidenced by its eigenvector in Table 6–5. The motion associated with this mode is a complex relationship between yaw and roll and angle of sideslip. The phases and magnitudes slightly differ from the motions of large aircraft; however, the dynamics are clearly dutch roll.

	Dutch Roll Mode	
	Magnitude	Phase
$\Delta\hat{v}$	0.2889	-133.8650^o
$\Delta\hat{p}$	4.9812	129.2711^o
$\Delta\hat{r}$	8.6632	153.8130^o
$\Delta\phi$	1.0000	0°
$\Delta\psi$	1.7392	24.5419^o

Table 6–5: Lateral-directional eigenvector

6.2 Modeling

6.2.1 Aerodynamic Modeling - Tornado

Modeling of flight dynamics was accomplished through the use of Tornado [20]. The output of this program contains all of the necessary stability derivatives, with the exception of $c_{m_{\dot{\alpha}}}$ to create a full set of linearized flight dynamics about a given state. All models discussed in this thesis were generated about a straight and level flight condition.

6.2.2 Rigid Body Modeling-ProE

The equations of motion contain moments of inertia that need to be determined in order to fully model the morphing aircraft. Actual airframes can undergo testing on a laser vibrometer to determine various structural and mass properties including moments of inertia. Analytical methods also exist. One such method is the creation of a finite element model. Such a model is a representation of the

structure made up many small individual members. This allows for the calculation of the needed moments of inertia about the center of gravity. ProE, a 3D modeling software package was used to generate the models. A finite element model of the base aircraft was created with articulated sections that were positioned at various points in the actuation range. Inertia tensors were calculated for each configuration. These varying parameters were fed into the LIV dynamics during simulations.

CHAPTER 7
APPLICATION-VARIABLE SPAN

7.1 Vehicle Description

The morphing concept explored here involves an airplane that has extensible wingtips with the capability of sliding in and out from underneath the inboard portion of the wing. The ability of the wing to maintain a consistent cross section throughout its range of motion is made possible by the use of a thin undercambered airfoil as is used by all of the MAV's at the University of Florida. The wingtips can articulate in unison to accommodate different portions of the flight envelope, or asymmetrically to facilitate roll control in lieu of aileron usage [**?**].

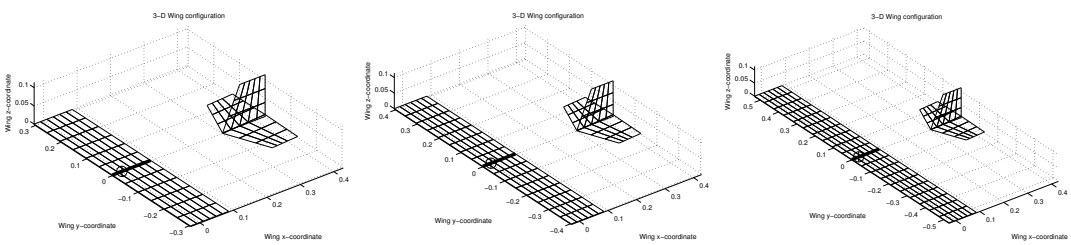

Figure 7–1: Morphing Span

7.2 Flight Dynamics

A set of LIV dynamics was generated for the span varying aircraft using Tornado. The dynamics were linearized about a straight and level flight condition with $\alpha = 5^o$ and $u = 12\ m/s$. The aircraft is observed to be at trim in Fig 7–2 at a span of 88 cm.

The damping ratio for the short period mode can be observed to be decreasing in Fig 7–3 as the span increases. There is a decreasing slope indicating an asymptotic approach to a bounded damping ratio.

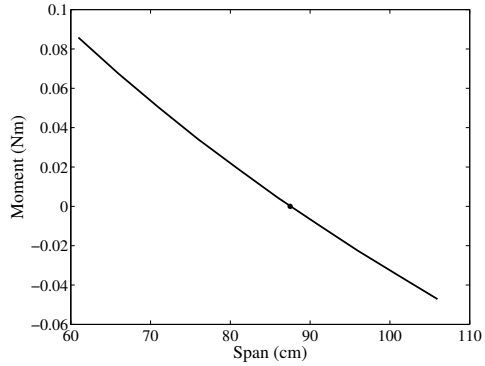

Figure 7–2: Pitching Moment Variation

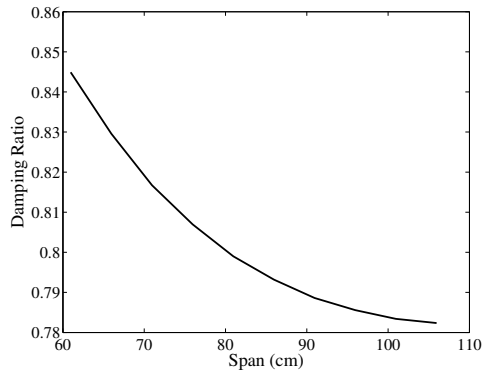

Figure 7–3: Short Period Damping Ratio Variation

The natural frequency of the short period mode steadily increases in an almost linear fashion in Fig 7–4. This corresponds to the expected destabilizing effect an increase in wing area would have while holding the tail volume coefficient constant. The horizontal tail's ability to stabilize the airplane decreases as wing is extended.

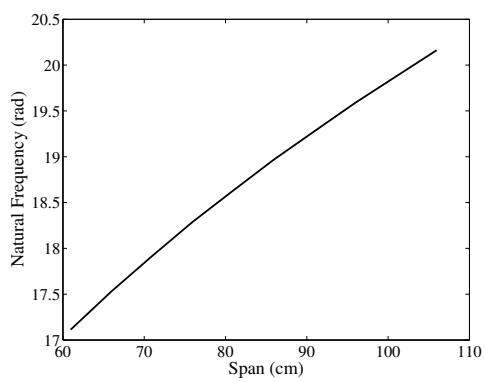

Figure 7–4: Short Period Frequency Variation

A look at the lightly damped phugoid mode reveals an opposite trend, which is shown in Fig 7–5. An increase in wing span increases damping. The frequency of the phugoid mode increases along with that of the short period mode, but with a lower over all change.

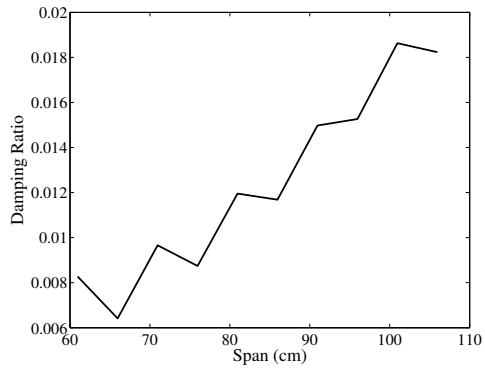

Figure 7–5: Phugoid Damping Ratio Variation

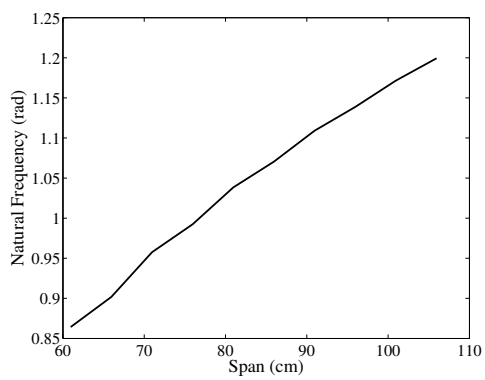

Figure 7–6: Phugoid Frequency Variation

Fig 7–7 shows the migration of the longitudinal modes over the range of spans. The short period mode is most affected, while the phugoid mode undergoes little variation in terms of a percentage change.

An increase in wing span serves to increase the dutch roll mode damping ratio as detailed in Fig 7–8 and to decrease its frequency as seen in Fig 7–9. Overall there is a destabilizing affect as the poles move slightly toward the imaginary axis in Fig 7–10.

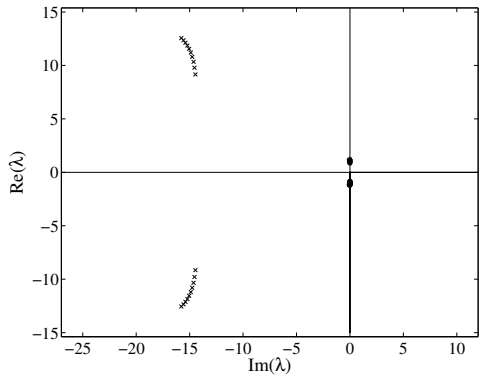

Figure 7–7: Pole Migration of Longitudinal Modes

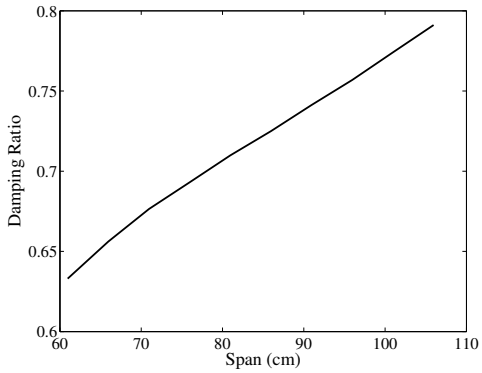

Figure 7–8: Dutch Roll Damping Ratio Variation

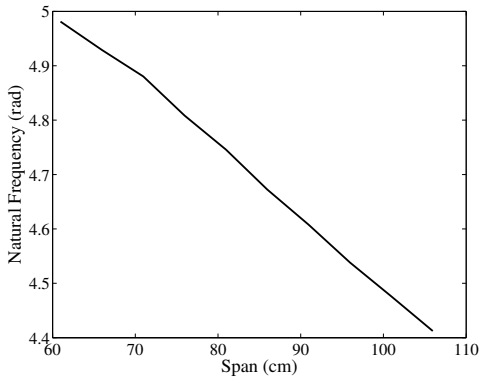

Figure 7–9: Dutch Roll Frequency Variation

Two disturbance rejection controllers were designed using *Lemma* 1 and *Lemma* 2. Gains are given in Table 7–1. Time response and span deflection plots appear in Fig 7–11. Both controllers improve upon the plants open loop response.

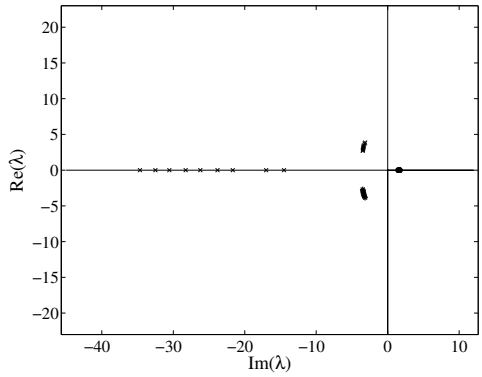

Figure 7–10: Pole Migration of Lateral Modes

	Lemma 1	Lemma 2	
	K	K_0	K_1
Δu	10	0	10000
Δw	10		10000
Δq	-10		-10000
$\Delta \theta$	-10		-10000

Table 7–1: Gains for span varying disturbance rejection controller

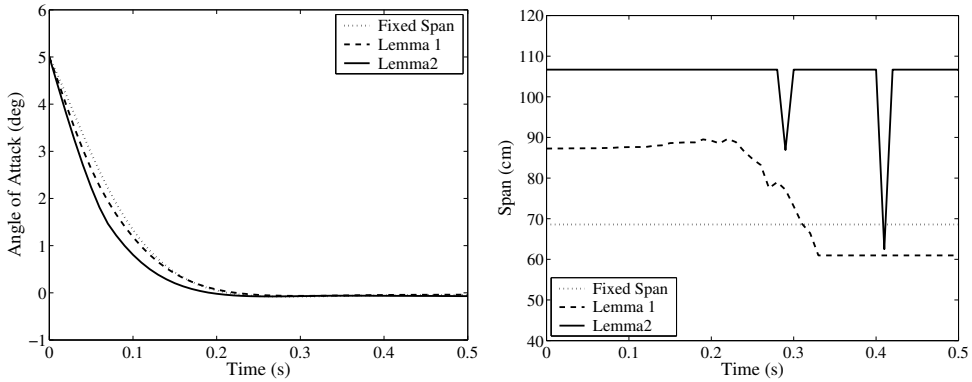

Figure 7–11: Pitch Response for Morphing Span

CHAPTER 8
APPLICATION-VARIABLE CAMBER

8.1 Vehicle Description

The usage of a thin undercambered airfoil section makes it considerably easier to affect a change in camber. A conventional wing has both upper and lower surfaces as well as internal structure to manipulate. A MMAV with a thin undercambered section can have its camber altered along the entire span of the wing with a single actuator. The theoretical wing on this airplane varies its camber in a precise way as the camber percentage changes in a linear manner [9]. If this design aspect was approached as a multi-disciplinary design optimization (MDDO) problem, the desired shape change would most likely be entirely different. This consideration is beyond the scope of this thesis, nor does the thesis intend to solve a MDDO problem [10, 22].

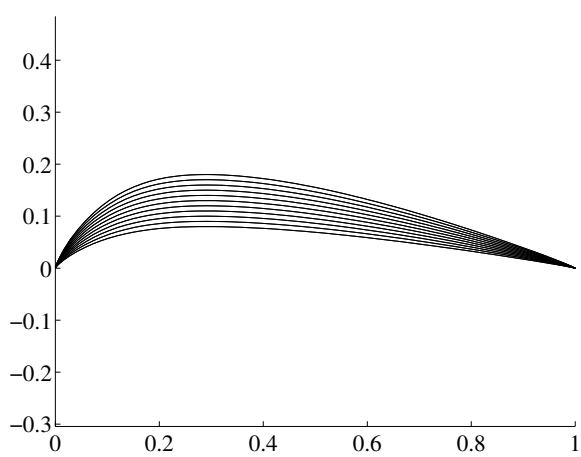

Figure 8–1: Morphing Camber

8.2 Flight Dynamics

Fig 8–2 is a plot of the pitching moment variation with camber change. There is no change in the pitching moment, requiring the use of elevator to trim out the airplane. This would indicate that camber is not a viable control effector for pitch control. Instead it may be more useful as a quasi-static flight envelope optimization technique.

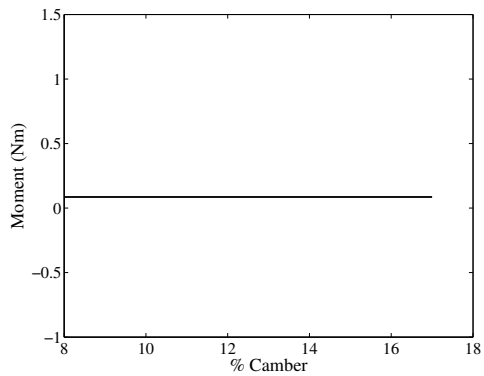

Figure 8–2: Pitching Moment Variation

Camber variations have little effect on the longitudinal dynamics. The short period is least affected, showing changes in damping ratio and frequency of only a few percent.

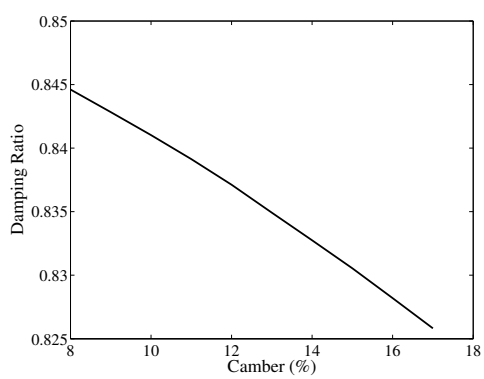

Figure 8–3: Short Period Damping Ratio Variation

The phugoid mode shows a slightly more marked change. An increase in camber correlates to increases in both damping ratio (Fig 8–5) and natural frequency (Fig 8–6).

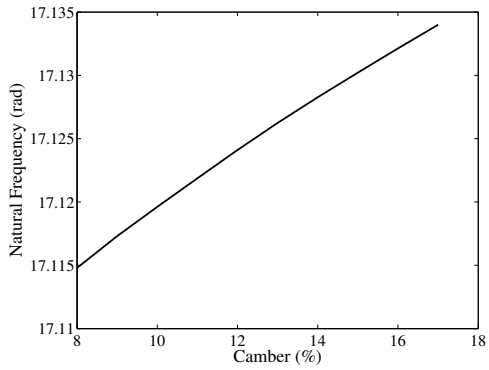

Figure 8–4: Short Period Frequency Variation

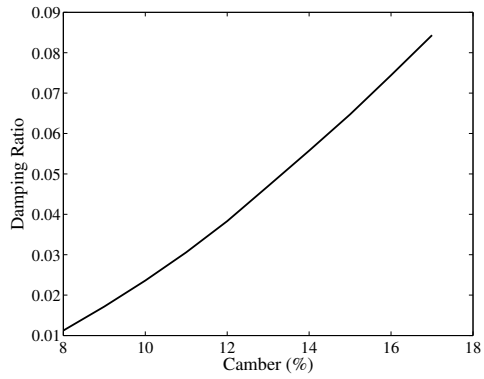

Figure 8–5: Phugoid Damping Ratio Variation

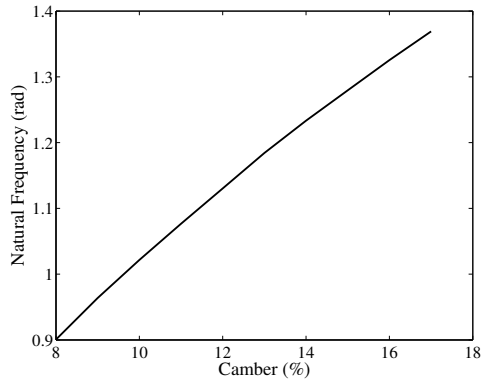

Figure 8–6: Phugoid Frequency Variation

Fig 8–7 displays the shift in pole due to a percent camber increase. Increasing the camber destabilizes the short period mode as the move a minute amount toward the imaginary axis. The phugoid mode in turn becomes slightly more stable. There is however no appreciable effect of camber change on the longitudinal modes.

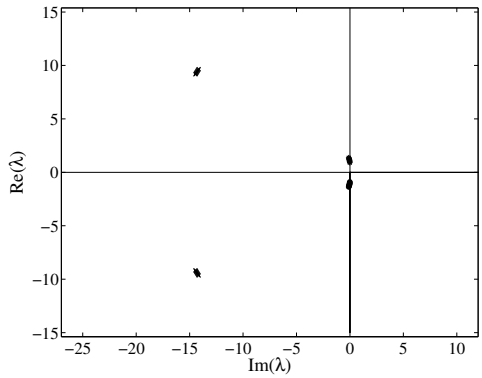

Figure 8–7: Pole Migration of Longitudinal Modes

An interesting result in the shift in lateral dynamics is the behavior of the damping ratio is observed in Fig 8–8. It initially decreases prior to reaching a minimum and then goes on to increase. The plot of the natural frequency in Fig 8–9 shoes a linear increasing trend.

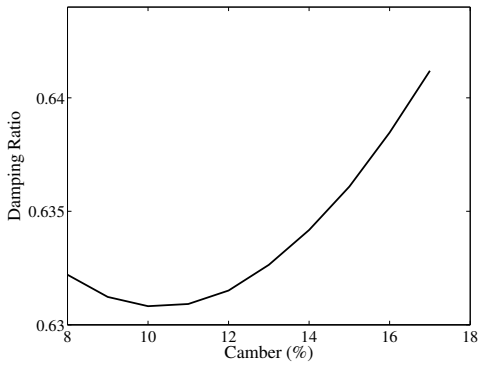

Figure 8–8: Dutch Roll Damping Ratio Variation

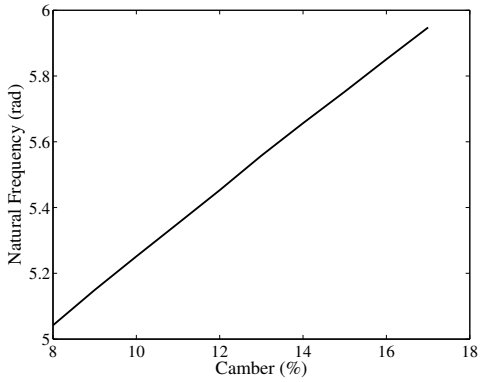

Figure 8–9: Dutch Roll Frequency Variation

Camber morphing has little effect on the lateral dynamics of the airplane also. The roll mode is destabilized by a small amount, while the dutch roll mode becomes more stable to some degree. An increase in camber moves the spiral pole away from the imaginary axis, making that mode yet more unstable.

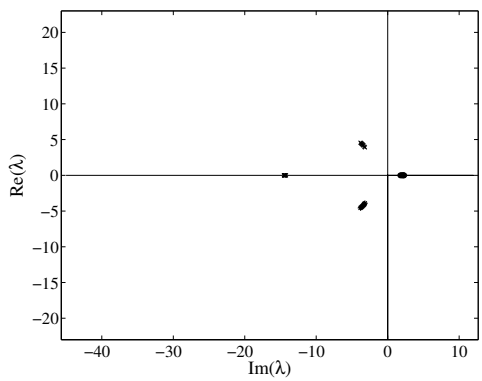

Figure 8–10: Pole Migration of Lateral Modes

Two disturbance rejection controllers were designed using *Lemma* 1 and *Lemma* 2. Gains are given in Table 8–1. Time response and span deflection plots appear in Fig 8–11. The 2 controllers closely match the openloop response of the aircraft, making only a small improvement.

	Lemma 1	Lemma 2	
	K	K_0	K_1
Δu	100	1500	10
Δw	10000		100
Δq	0		-10
$\Delta\theta$	-1		-10

Table 8–1: Gains for camber varying disturbance rejection controller

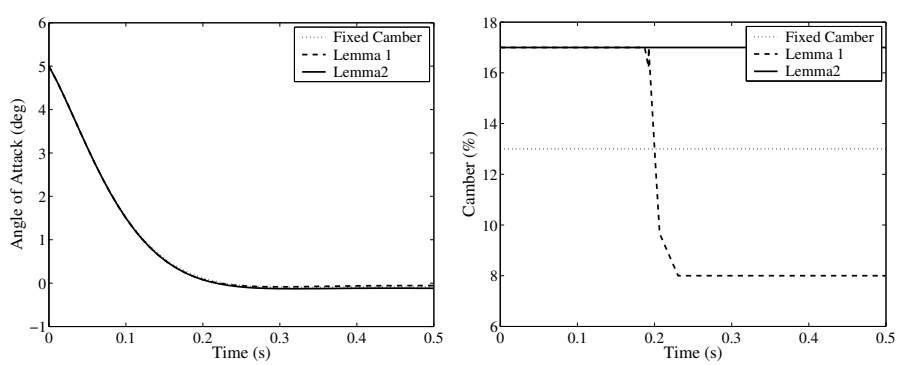

Figure 8–11: Pitch Response for Morphing Camber

CHAPTER 9
APPLICATION-VARIABLE CHORD

9.1 Vehicle Description

The vehicle proposed here has a portion of the wing which slides out in order to increase the wing area, much like the span varying case. This is not unlike a Fowler flap except for the greater range of motion. This MMAV concept has the capability to double its chord length.

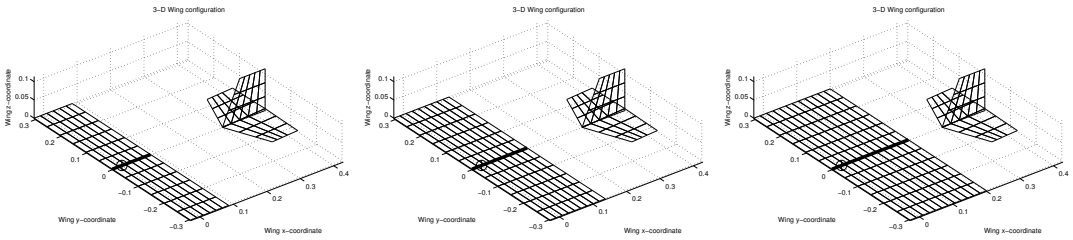

Figure 9–1: Morphing Chord

9.2 Flight Dynamics

Fig 9–2 plots the pitching moment against a change in chord. It can be noted that a significant moment is created by morphing the chord. This makes sense as it is expected that a large change in the chord would have pronounced effect on the pitching moment. The neutral point of a wing usually lies at about the 50gravity remains at roughly the same point, depending on the mass of the wing relative to the rest of the airframe.

This theme of large longitudinal effects by chord variations continues in the dynamics. Fig 9–3 shows how the short period damping ratio quickly increases to a maximum of one at which point it becomes two separate convergences.

The phugoid mode of the aircraft is affected to a lesser extent by a change in chord. The modal properties are still more sensitive to this form of morphing than

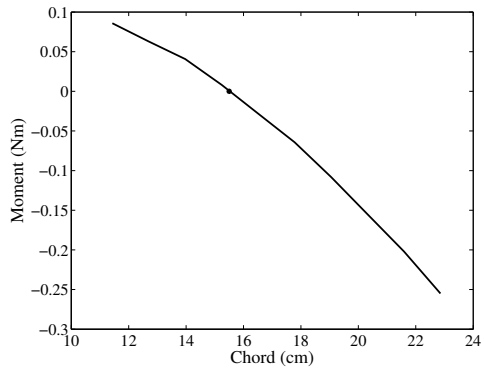

Figure 9–2: Pitching Moment Variation

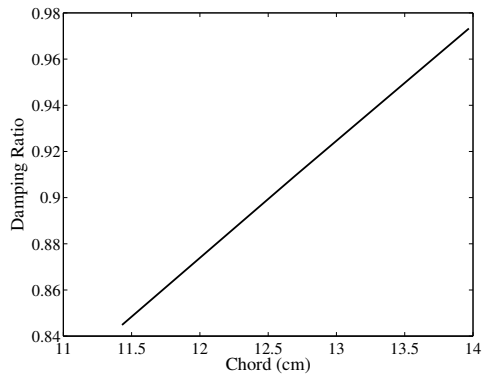

Figure 9–3: Short Period Damping Ratio Variation

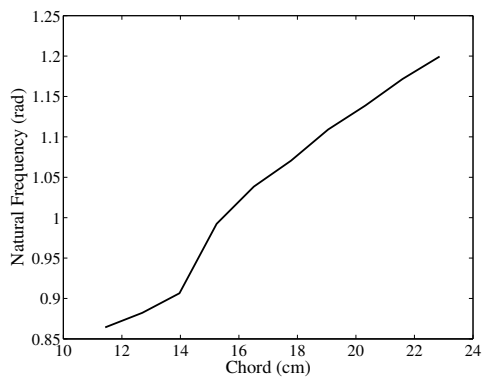

Figure 9–4: Short Period Frequency Variation

to the previous two. Figs 9–5 and 9–6 show increases in the phugoid damping ratio and frequency, respectively.

The movement of the longitudinal poles due to a change in chord is given in Fig 9–7. The short period mode breaks down into two separate convergences, one of which continues to grow more stable, with the other moving toward the imaginary axis. The phugoid mode grows more stable with an increase in chord.

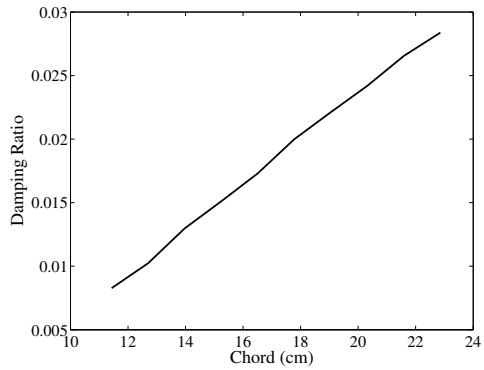

Figure 9–5: Phugoid Damping Ratio Variation

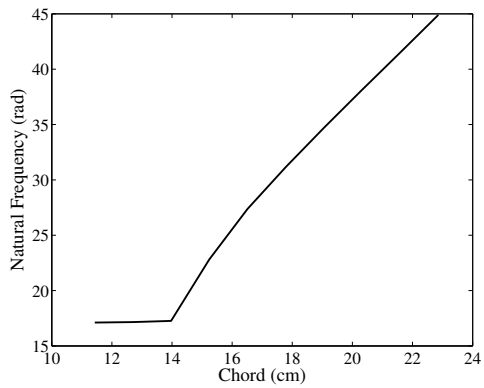

Figure 9–6: Phugoid Frequency Variation

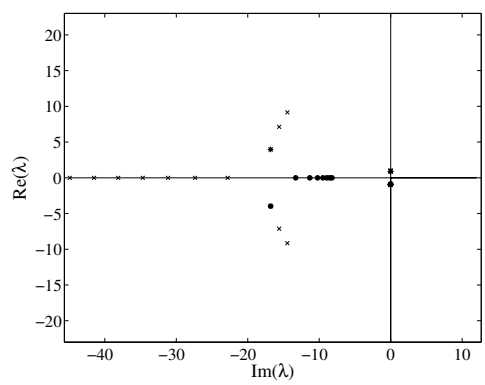

Figure 9–7: Pole Migration of Longitudinal Modes

Figs 9–8 and 9–9 show the damping ratio and the natural frequency of the dutch roll 0mode following the same oscillatory pattern, with a globally decreasing trend.

Lateral pole migration due to a change in chord is given in Fig 9–10. The roll convergence grows more stable as the chord increases and the spiral divergence becomes even less stable.

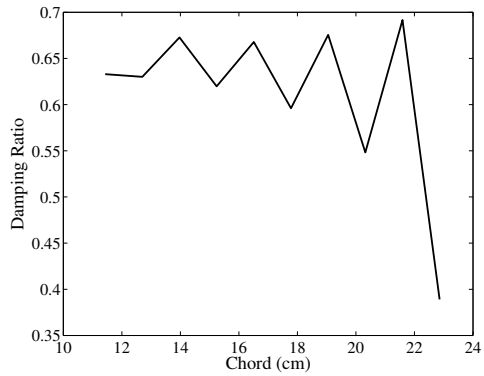

Figure 9–8: Dutch Roll Damping Ratio Variation

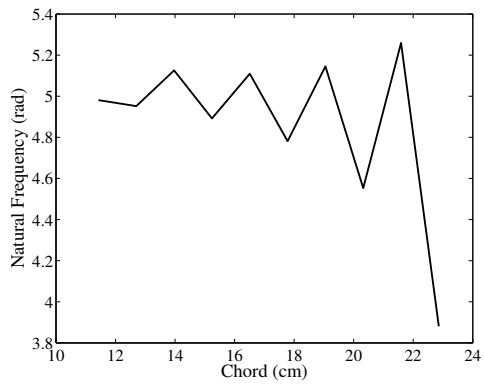

Figure 9–9: Dutch Roll Frequency Variation

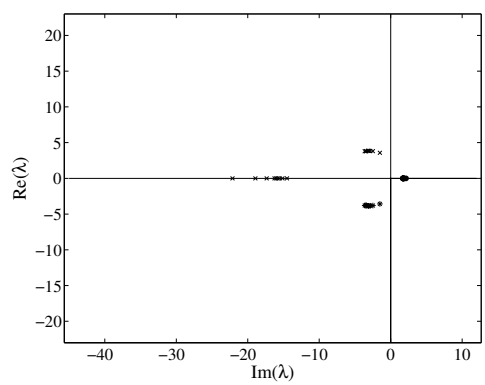

Figure 9–10: Pole Migration of Lateral Modes

Two disturbance rejection controllers were designed using *Lemma* 1 and *Lemma* 2. Gains are given in Table 9–1. Time response and span deflection plots appear in Fig 9–11. Morphing chord has the greatest authority over pitch response of any of the types of morphing considered in this thesis.

	Lemma 1	Lemma 2	
	K	K_0	K_1
Δu	1	0	10
Δw	100		10
Δq	-1		-10
$\Delta \theta$	-1		-10

Table 9–1: Gains for chord varying disturbance rejection controller

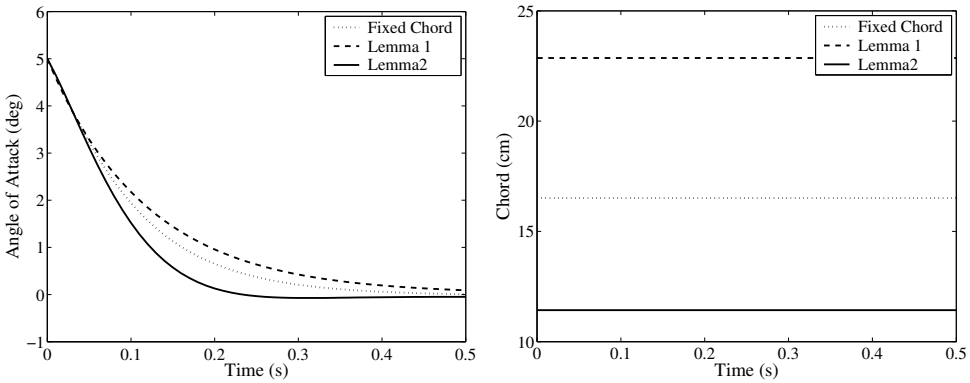

Figure 9–11: Pitch Response for Morphing Chord

REFERENCES

[1] Abdulrahim, M., Garcia, H., and Lind, R., "Flight Characteristics of Wing Shaping for a Micro Air Vehicle with Membrane Wings," *In press, AIAA Journal Aircraft.*

[2] M. Amprikidis and J.E. Cooper, "Development of Smart Spars for Active Aeroelastic Structures," *AIAA Structures, Dynamics, and Materials*, AIAA-2003-1799, Norfolk, VA, April 2003.

[3] J. Blondeau, J. Richeson and D.J. Pines, "Design, Development and Testing of a Morphing Aspect Ratio Wing using an Inflatable Telescopic Spar," *AIAA Structures, Dynamics, and Materials*, AIAA-2003-1718, Norfolk, VA, April 2003.

[4] Boothe, K., Fitzpatrick, K., and Lind, R., "Controllers for Disturbance Rejection for a Linear Input-Varying Class of Morphing Aircraft,"*Submitted to the AIAA/ASME/ASCE/AHS Structures, Structural Dynamics, and Materials Conference*, Austin, TX, April 2005.

[5] J. Bowman, B. Sanders and T. Weisshar, "Evaluating the Impact of Morphing Technologies on Aircraft Performance," *Proceedings of the AIAA Structures, Structural Dynamics and Materials Conference*, AIAA-2002-1631, Denver, CO, April 2002.

[6] P. Bugsby, *First to Fly: How Wilbur and Orville Wright Invented the Airplane*, Crown Books, New York, NY, March 2003.

[7] D. Cadogan, T. Smith, R. Lee and S. Scarborough, "Inflatable and Rigidizable Wing Components for Unmanned Aerial Vehicles," *Proceedings of the AIAA Structures, Structural Dynamics and Materials Conference*, AIAA-2003-1801, Norfolk, VA, April 2003.

[8] J.B. Davidson, P. Chwalowski, and B.S. Lazos, "Flight Dynamic Simulation Assessment of a Morphable Hyper-Elliptic Cambered Span Winged Configuration," *Proceedings of the AIAA Structures, Structural Dynamics and Materials Conference*, AIAA-2003-5301, Norfolk, VA, August 2003.

[9] M. Drela, "Xfoil 6.94," CFD Software, Massachusetts Institute of Technology Massachussets, 2001.

[10] S. E. Gano. J. E. Renaud, S. M. Batill, A. Tovar, "Shape Optimization for Conforming Airfoil," *Proceedings of the AIAA/ASME/ASCE/AHS Structures,*

Structural Dynamics, and Materials Conference, AIAA 2003-1579, Norfolk, VA, April 2003.

[11] H. Garcia, M. Abdulrahim, and R. Lind, "Roll Control for a Micro Air Vehicle using Active Wing Morphing," *Proceedings of the AIAA Guidance, Navigation and Control Conference*, AIAA-2003-5347, San Antonio, TX, 2003.

[12] P.G. Ifju, S. Ettinger, D.A. Jenkins and L. Martinez, "Composite Materials for Micro Air Vehicles" *Proceedings of the Society for Advancement of Materials and Process Engineering Annual Conference*, Long Beach, CA, May 2001.

[13] J. Jackowski, K. Boothe, R. Lind, and P. Ifju, "Modeling the Flight Dynamics of a Micro Air Vehicle," *Proceedings of the European Micro Air Vehicle Conference*, Braunschweig, Germany, July 2004.

[14] C.O. Johnston, D.A. Neal, L.D. Wiggins, H.H. Robertshaw, W.H. Mason and D.J. Inman, "A Model to Compare the Flight Control Energy Requirements of Morphing and Conventionally Actuated Wings," *Proceedings of the AIAA/ASME/AHS Adaptive Structures Conference*, AIAA-2003-1716, Norfolk, VA, August 2003.

[15] J. Kehoe, R. Causey, R. Lind, and A.J. Kurdila,"Maneuvering and Tracking for a Micro Air Vehicle using Vision-Based Feedback," *World Aviation Congress*, November 2004.

[16] J. Kehoe, J.W. Grzywna, R. Causey, J. Plew, M. Abdulrahim, M.C. Nechyba, and R. Lind, "Waypoint Navigation for a Micro Air Vehicle using Vision-Based Attitude Estimation," *Proceedings of the European Micro Air Vehicle Conference*, Braunschweig, Germany, July 2004.

[17] Y. Lian and W. Shyy, "Three-Dimensional Fluid-Structure Interactions of a Membrane Wing for Micro Air Vehicle Applications," *Proceedings of the AIAA Structures, Structural Dynamics and Materials Conference*, AIAA-2003-1726, Norfolk, VA, April 2003.

[18] R. Lind, M. Abdulrahim, K. Boothe, and P. Ifju, "Morphing for Flight Control of a Micro Air Vehicles," *Proceedings of the European Micro Air Vehicle Conference,*, Braunschweig, Germany, July 2004.

[19] H. J. Marquez, *Nonlinear Control Systems*, John Wiley and Sons, Hoboken, NJ, May 2003.

[20] T. Melin, "A Vortex Lattice MATLAB Implementation for Linear Aerodynamic Wing Applications," Master's Thesis, Royal Institute of Technology(KTH), 2000.

[21] R.C. Nelson, *Flight Stability and Automatic Control*, McGraw-Hill, New York, NY, March 1998.

[22] S.L. Padula, J.L. Rogers, and D.L. Raney, "Multidisciplinary Techniques and Novel Aircraft Control Systems," **th AIAA/NASA/USAF/ISSMO Multidisciplinary Analysis and Optimization Symposium,* AIAA 2000-4848, Long Beach, CA, September 2000.

[23] M. Park, L.Green, R.C. Montgomery, and D.L. Raney, "Determination of Stability and Control Derivatives Using Computational Fluid Dynamics and Automatic Differentiation," *17th AIAA Applied Aerodynamics Conference,* AIAA 99-3136, Norfolk, VA, June 1999.

[24] H.F. Parker, "The Parker variable Camber Wing," *Report # 77, from the Fifth Annual Report, National Advisory Committee for Aeronautics* Washington, DC, 1920.

[25] D.L. Raney, R.C. Montgomery, L.L. Greeen, and M.A. Park, "Flight Control Using Distributed Shape-Change Effector Arrays," *Proceedings of the AIAA/AME/ASCE/AHS/ASC Sructures, Stuctural Dynamics, and Materials Conference and Exhibit,* AIAA 2000-1560, Atlanta, GA, April 2000.

[26] t B. Sanders, F.E. Eastep and E. Forster, "Aerodynamic and Aeroelastic Characteristics of Wings with Conformal Control Surfaces for Morphing Aircraft," *Journal of Aircraft*, Vol. 40, No. 1, January-February 2003.

[27] V.B. Shavrov, *History of Aircraft Construction in the USSR*, Russian Aeronautical Education Series Publishers, Moscow, Russia, August 1968.

[28] D. Viieru, Y. Lian, W. Shyy and P. Ifju, "Investigation of Tip Vortex on Aerodynamic Performance of a Micro Air Vehicle," AIAA-2003-3597, 2003.

[29] M.R. Waszak, J.B. Davidson, and P.G. Ifju, "Simulation and Flight Control of an Aeroelastic Fixed Wing Micro Air Vehicle," AIAA-2002-4875, August 2002.

[30] M.R. Waszak, L.N. Jenkins, and P.G. Ifju, "Stability and Control Properties of an Aeroelastic Fixed Wing Micro Air Vehicle," AIAA-2001-4005, August 2001.

[31] R.W. Wlexien, G.C. Horner, A.R. McGowan, S.L. Padula, M.A. Scott, R.J. Silcox, and J.O. Simpson, "The Aircraft Morphing Program," *AIAA Meeting Paper* AIAA-98-1927 1998.

[32] T.R. Yechout, S.L. Morris, D.E. Bossert, and W.F. Hallgren, *Introduction to Aircraft Flight Mechanics*, American Institute of Aeronautics and Astronautics, Reston, VA, September 2003.

BIOGRAPHICAL SKETCH

Kenneth Boothe was born in Pensacola, Florida, on February 2, 1974 where he spent most of his life prior to coming to Gainesville in January of 1998 to attend the University of Florida. While in Pensacola, Kenneth graduated at the top of his high school class and went on to study computer science the University of West Florida on a scholarship. He continued taking classes sporadically while working in a variety of jobs including restaurant manager, white water raft guide, and a partnership in a small landscaping business. Kenneth decided to return to school to earn a degree in aerospace engineering in accordance with a life long interest in aviation. This interest was spawned by a teacher in a a gifted program he was involved in during his youth. Mr. Rod Smith offered a class entitled simply "Flight." The fundamental forces of flight were introduced and some experiments were performed with small styrofoam models placed in front of a fan. Kenneth earned his BS in aerospace engineering in 2003 and hopes to earn his MS in the same discipline in 2004.